

# Effect of Blade Angle and Number on the Performance of Bánki Hydro-Turbines: Assessment using CFD and FDA Approaches

Dandun Mahesa Prabowoputra

Department of Industrial Engineering, Universitas Jenderal Soedirman

Aditya Rio Prabowo

Department of Mechanical Engineering, Universitas Sebelas Maret

Yaningsih, Indri

Department of Mechanical Engineering, Universitas Sebelas Maret

Dominicus Danardono Dwi Prija Tjahjana

Department of Mechanical Engineering, Universitas Sebelas Maret

他

<https://doi.org/10.5109/6782156>

---

出版情報 : Evergreen. 10 (1), pp.519-530, 2023-03. 九州大学グリーンテクノロジー研究教育センター  
バージョン :

権利関係 : Creative Commons Attribution-NonCommercial 4.0 International



# Effect of Blade Angle and Number on the Performance of Bánki Hydro-Turbines: Assessment using CFD and FDA Approaches

Dandun Mahesa Prabowoputra<sup>1</sup>, Aditya Rio Prabowo<sup>2,\*</sup>, Indri Yaningsih<sup>2</sup>,  
Dominicus Danardono Dwi Prija Tjahjana<sup>2</sup>, Fajar Budi Laksono<sup>2,3</sup>,  
Ristiyanto Adiputra<sup>4</sup>, Hendri Suryanto<sup>3</sup>

<sup>1</sup>Department of Industrial Engineering, Universitas Jenderal Soedirman, Purbalingga 53122, Indonesia

<sup>2</sup>Department of Mechanical Engineering, Universitas Sebelas Maret, Surakarta 57126, Indonesia

<sup>3</sup>Department of Research and Development, DTECH Inovasi Indonesia Co. Ltd., Salatiga 50742, Indonesia

<sup>4</sup>Research Center for Hydrodynamics Technology, National Research and Innovation Agency (BRIN),  
Surabaya 60112, Indonesia

\*Author to whom correspondence should be addressed:

E-mail: aditya@ft.uns.ac.id

(Received February 27, 2023; Revised March 24, 2023; accepted March 24, 2023).

**Abstract:** The Bánki turbine is a cross-flow turbine with a simple structure that is easy to modify. Changing the turbine's runner geometry is one of the modifications that have an effect on its performance. The goal of this study is to quantify the effect of increasing number of blades and the angle of the blades on the performance of the Bánki turbine. This study was carried out using three-dimensional modeling with the ANSYS CFX device and the computational fluid dynamics (CFD) method. The five angles of the blade, namely 10°, 15°, 20°, 25°, and 30°, are used to create variations. In addition to the angle factor of the blade, research has been conducted on the number of blades, which are 12 blades, 16 blades, 20 blades, 24 blades, 32 blades, 36 blades, 40 blades, 48 blades, and 52 blades. In a steady-state modeling condition, the applied boundary condition is a water flow velocity of 3 m/s. The results of the CFD modeling are analyzed using a factorial design analysis (FDA). The results indicate that runners with a 15° Blade's angle and 40-blade perform best. Results of the factorial design analysis show that the blade angle factor and the number of blades interact.

Keywords: Bánki-Turbine; Hydro-Turbine; Computational Fluid Dynamics; Factorial Design

## 1. Introduction

The turbine is an important component in converting hydro energy to electrical energy. With so much hydropower in Indonesia, research into improving hydro turbine performance is critical. In 2020, Indonesia's hydropower potential was estimated to be around 75,000 MW<sup>1)</sup>. Cross-flow turbines, such as Savonius turbines<sup>2)</sup> and Bánki turbines<sup>3)</sup>, have simple structures.

The straightforward construction of a cross-flow type turbine is very alluring to researchers for the purpose of development. The next stage of development for one variety of cross-flow turbines is an investigation into the nature of the component's structure<sup>4)</sup>. Based on the findings of other studies, the geometry of the turbine is one of the critical factors in determining the overall structure of the turbine. The aspect ratio, overlap ratio, number of blades, number of stages, and the shape of the blade are some of the geometric factors that influence the

turbine<sup>5)</sup>. Several types of research have been done on Bánki turbines to discover the phenomena and efforts to improve Bánki turbine performance. Experimental methods have been analyzed to determine the effect of the blade tip shape on Bánki turbine runners. The study showed that blades with blunt ends produced the best performance<sup>6, 7)</sup>. The number of blades in the runner geometry influences Bánki turbine performance<sup>8)</sup>. As a result, the geometric factor affects the performance of the Bánki turbine. The performance of hydro turbines is studied using various methods, including experimental approaches<sup>9)</sup> and computational fluid dynamics<sup>10)</sup>. The water jet powers the atmospheric radial flow wheel Bánki turbine. The Bánki turbine has a nozzle and Runner. Two parallel circular disks joined by curved blades form the Runner<sup>11)</sup>. The Bánki turbine benefits from a simple structure and operation<sup>6)</sup>. This advantage makes Bánki turbines more suitable for increasing renewable energy

processing<sup>3)</sup>. However, researchers have only looked at one type of geometry change factor in Bánki runners to see how it affects them. It is possible that changing several variables will have more significant impact on turbine performance, resulting in an optimal design.

Research has been carried out on Bánki turbines with the computational fluid dynamics (CFD) method in three dimensions. This research was carried out with a variation of two factors: the angle of the blade and the number of blades on the Runner. The purpose of this research that has been done is to find out the two geometric factors on the performance of the Bánki turbine. Therefore, through this research, the design of the blade angle can be obtained that can produce the best performance. Then, the results of this research were carried out by factorial design analysis (FDA), where this analysis can be applied to determine the interaction between factors<sup>12)</sup>. Studies conducted by previous researchers did not use FDA analysis. This FDA analysis is used to strengthen the analysis of the influence of each factor on the performance of the Bánki turbine.

## 2. Literature Review

Cross-flow turbines are one type of turbine that has been popular in several studies. In general, cross-flow turbines have the advantage of having a simple structure and easy maintenance. These advantages make cross-flow turbines easy to modify<sup>3)</sup>.

One subclass of cross-flow turbines is known as a Bánki turbine. Donat Bánki was the first person to propose the idea of a Bánki-type cross-flow turbine back in 1917. The idea was later developed further by Mockmore and Merryfield in their research conducted in 1949<sup>6)</sup>. The nozzle and the runner make up the two primary components that constitute the Bánki turbine. The runner is made up of two discs that are the same size and shape and are joined at the edge by curved blades and hoverers. The nozzle, which has a rectangular cross-section, directs the water jet toward the runner. The water then hits the blades on the rim, flows into the channels between the blades for the first time, flows through the empty space in the middle of the runner, and flows through the mid-blade channels for a second time before almost radiating out of the runner<sup>13)</sup>.

On the overall performance of the cross-flow turbine, the geometry factor has a significant impact. The performance of the turbine is affected by the number of blades; the studies conducted with 32 blades, 36 blades, 40 blades, 44 blades, and 48 blades all found that the runner with 40 blades achieved the highest level of performance. The  $C_{p_{max}}$  that was arrived at as a result is 20.4%<sup>8)</sup>. Alterations to the profile of the blades can also have an impact on the overall performance of the turbine. The performance of the turbine can be improved by 8–11% simply by changing the profile of the blades<sup>7)</sup>.

There are many steps involved in modeling-based research, but some of the most crucial are the mesh study, benchmarking, meshing, and boundary condition

determination processes. The zone is typically split in two for modeling purposes: the rotating zone, where conditions such as rotational speed limits apply, and the stationary zone, where such limits do not apply<sup>5)</sup>. The optimal number of meshes for the modeling process can be found through mesh study. Adjusting the mesh size changes the total number of mesh elements in the object, which is a necessary step in the mesh study process<sup>8)</sup>.

The modeling that has been done has several outputs, one of which is the torque value. The torque value is one of the input values to obtain the performance value of the turbine Bánki under study. The Coefficient of Power value indicates the turbine Bánki performance. Equations 1 to 3 shows the calculation. The following are the given equations<sup>14)</sup>:

$$C_p = \frac{P_{runner}}{P_{Available}} \quad (1)$$

$$P_{Available} = 0,5 \times \rho \times A \times V^3 \quad (2)$$

$$P_{Runner} = T \times \frac{2\pi n}{60} \quad (3)$$

One of the stages in the modeling process is benchmarking or validating with other similar studies. At this stage, the error value will be obtained using Equation 4. where the formula is as follows<sup>15)</sup>:

$$error = \frac{1}{n} \sum_{i=1}^n |f_i - y_i| \quad (4)$$

The performance value of each runner is analyzed using a factorial design. The effect of the factor of the number of blades on the runner and the angle of the blade on the runner will be investigated. The analysis uses the calculation shown by Equations 5-9, the data from the calculation results are presented in Table 2<sup>16)</sup>:

$$SS_A = \frac{1}{bn} \sum_{i=1}^a y_{i..}^2 - \frac{y_{...}^2}{abn} \quad (5)$$

$$SS_B = \frac{1}{an} \sum_{j=1}^b y_{.j.}^2 - \frac{y_{...}^2}{abn} \quad (6)$$

$$SS_{Subtotal} = \frac{1}{n} \sum_{i=1}^a \sum_{j=1}^b y_{ij.}^2 - \frac{y_{...}^2}{abn} \quad (7)$$

$$SS_{AB} = SS_{Subtotal} - SS_A - SS_B \quad (8)$$

$$SS_E = SS_T - SS_{Subtotal} \quad (9)$$

In this equation, notations A and B are symbols of the factors being analyzed. The symbols A and B will be replaced with the factor names. For example, if the factors used are speed and geometry, symbol A is replaced with Velocity, and symbol B is replaced with Geometry. In comparison, AB notation is used to determine the interaction between factor A and factor B<sup>15)</sup>. The application of this analysis can be used to determine the interaction between factors such as pressure and temperature factors in the production of biodiesel<sup>17)</sup>, the effect of the blades on the turbine Bánki<sup>18)</sup>, or the geometry factor and TSR on the performance of the savonius turbine<sup>19)</sup>.

Table 2. calculation results of factorial design<sup>16)</sup>.

Variation	SS	DOF	Mean Square	F <sub>0</sub>
Factor A	SS <sub>A</sub>	a-1	$MS_A = \frac{SS_A}{a-1}$	$F_0 = \frac{MS_A}{MS_E}$
Factor B	SS <sub>B</sub>	b-1	$MS_B = \frac{SS_B}{b-1}$	$F_0 = \frac{MS_B}{MS_E}$
Interaction A B	SS <sub>AB</sub>	(a-1)(b-1)	$MS_{AB} = \frac{SS_{AB}}{(a-1)(b-1)}$	$F_0 = \frac{MS_{AB}}{MS_E}$
Error	SS <sub>E</sub>	Ab(n-1)	$MS_E = \frac{SS_E}{ab(n-1)}$	
Total	SS <sub>T</sub>	Abn-1		

### 3. Design of Runner

This research has been carried out on turbine Bánki with variations in the geometry of the runners. The geometric factors whose influence was studied in the analysis were the number of blades and the angles on the blades. Fig. 1 shows the isometric design of the Runner on the Bánki and a cutout to show the shape of the blades. The dimensions used are shown in Table 1, and a description of the geometric dimensions is given in Figs. 1 to 4. The dimensions and shape of this Runner are based on previous research, which only applied an angle of 20, and a number of blades<sup>8)</sup>.

Table 1. Dimension of Runner on Bánki turbine.

No	Symbol	Note	Dimension
1.	D <sub>1</sub>	Outer Diameter Runner	80 mm
2.	D <sub>2</sub>	Inner Diameter Runner	60 mm
3.	R <sub>r</sub>	Radius	10 mm
4.	t	Thickness	1.5 mm
5.	H	High of Runner	130 mm
6.	Θ	Angle	10°, 20°, 30°

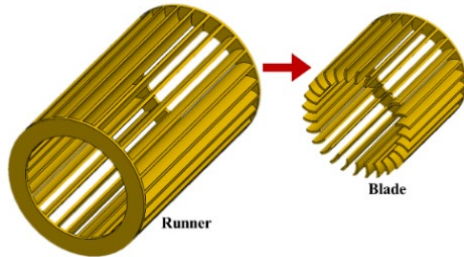


Fig. 1: Geometry Design of Bánki Turbine.

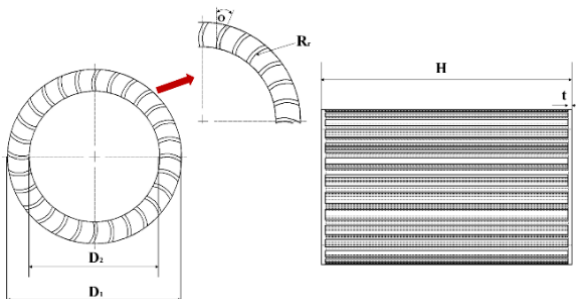


Fig. 2: Symbol on Dimension of Bánki's Runner.

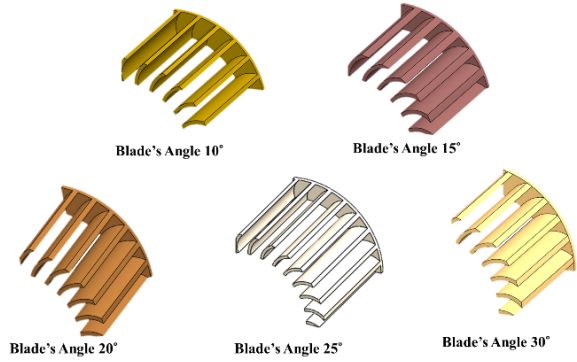


Fig. 3: 3D Cropping of Runner's geometry in Blade's angle Variation.

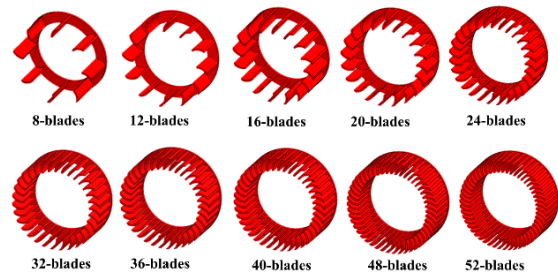
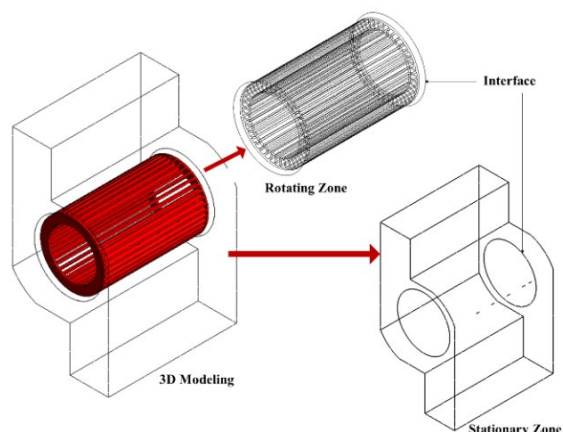


Fig. 4: 3D Cropping of Runner's geometry in Number of Blade Variation.

The research that has been done is applied to 5 angle variations, and for each angle variation, 10 variations of the number of blades are used. So this research was conducted on 50 runners. Fig. 3 shows a sectional image of the Runner at various angles belonging to the angles 10°, 15°, 20°, 25°, and 30°. Then for each angle variation on the blade, there are 12 variations in the number of blades, as shown in Fig. 4. The variations in the number of blades are 8-blades, 12-blades, 16-blades, 20-blades, 24-blades, 32-blades, 36-blades, 40-blades, 48-blades and 52-blade.

### 4. Modeling Method

The analysis of the Bánki turbine has been carried out in a modeling manner using the computational fluid dynamics method. This research has been conducted with three-dimensional modeling. The software used to conduct this research is ANSYS CFX. This model is divided into two zones, namely the stationary zone and the rotary zone. The division of the model into two zones is usually done in water turbine modeling<sup>20, 21)</sup>. Fig. 5 shows the distribution of zones in the modeling that has been done. The two zones are connected by an interface. The meshing processes for the two zones have been carried out separately but with the same settings.



**Fig. 5:** Zone in 3D Modeling of Bánki Turbine.

The results of the meshing process in the stationary and rotary zones are shown in Fig. 6. A tetrahedron mesh has been used. Because it can achieve the curved shape of the rotor, this tetrahedron is commonly used in water turbine modeling cases<sup>22</sup>. Use inflation during the meshing process to get closer to the rotor for more detail<sup>23</sup>. To obtain the best mesh, the meshing process is repeated several times. Mesh study refers to the process of determining the best mesh. Changing the mesh size is used in this mesh study<sup>24, 25</sup>. During the mesh study process, up to eight size settings were made. The mesh study results are depicted in the graph in Fig. 7a.

Fig. 7b is a graph depicting the results of benchmarking between the model and Makarim's research<sup>26</sup>. Equation 4 reveals an error value of 6% for the results. This error is acceptable, as the maximum allowable error for the computational fluids method is 10%<sup>20, 27</sup>.

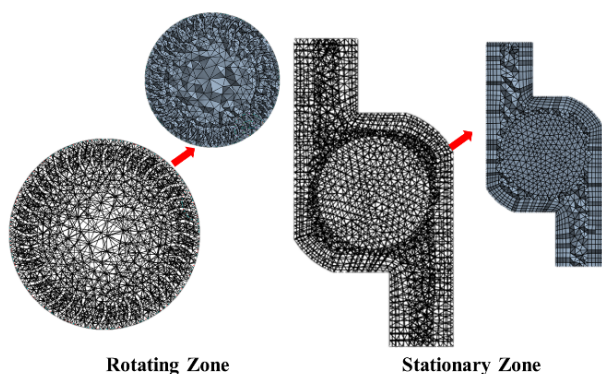
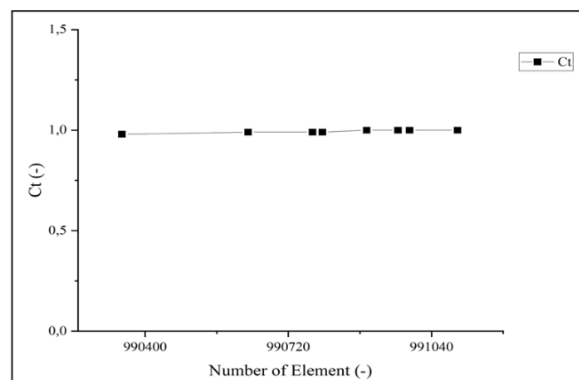
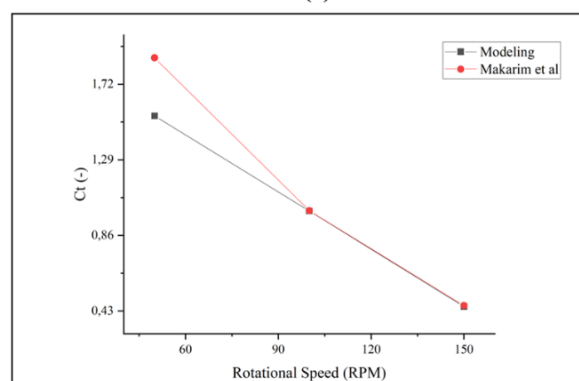


**Fig. 6:** Meshing result of rotating and stationary zone.



**(a)**



**(b)**

**Fig. 7:** Summarized results: a) Mesh Study, and b) benchmarking modeling with makarim research<sup>25</sup>.

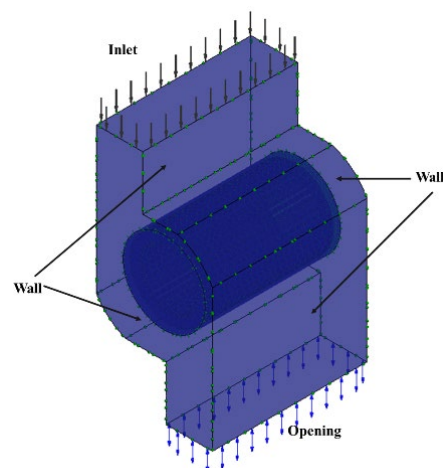


**Fig. 8:** Scheme of computational fluid dynamics modelling.

Boundary conditions apply to stationary and rotary zones. The rotational speed is a boundary condition in the rotary zone. The rotational speed used is 50–450 rpm. In the stationary zone, there are several boundary conditions, including inlets, outlets, and walls. The inlet boundary condition used is the incoming fluid velocity, which is 3 m/s<sup>12</sup>. The boundary conditions at the outlet have used the opening boundary condition type<sup>28</sup>. The condition used is a static pressure of 1 atm<sup>29</sup>. The next boundary condition is the wall, where the wall uses the no-slip condition<sup>30</sup>. The connection between the rotating zone and the

stationary zone uses the fluids-to-fluids interface and the frozen rotor type<sup>8)</sup>. The schematic is shown in Fig. 8. The modeling was carried out under steady-state conditions<sup>19,31)</sup> with a residual value of  $10^{-3}$ . The turbulent type used was shear-share transport<sup>20)</sup>.

## 5. Result an Discussion

The modeling that has been done produces output in the form of torque values, pressure contours, velocity contours, and velocity vectors. This value is converted to the Coefficient of power using Equations 1 to 3. So the graph shows the relationship between Rotational Speed and Coefficient of power. The results of this study include the effect of the number of blades on Bánki turbine performance at each blade angle variation and comparing  $C_{p_{max}}$  at the best number of blades with the blade angle variation factor.

The performance of the turbine Bánki with an angle of  $10^\circ$  is shown in Fig. 9. The results show a positive value at the rotational speed interval of 50 – 300 rpm. The  $C_{p_{max}}$  values for each blade sequentially from 8-blades to 52-blades were 0.092, 0.087, 0.095, 0.102, 0.127, 0.143, 0.167, 0.178, 0.140, and 0.112. in the 8-blades to 20-blade variations, it will reach  $C_{p_{max}}$  at a rotational speed of 100 rpm. After that, the  $C_p$  value decreases. Whereas the 24-blades to 52-blades variations will reach  $C_{p_{max}}$  at a rotational speed of 150 rpm, the  $C_p$  will reduce. The 36-

blade and 40-blade variations have a longer rotational speed interval than the other variations. In general, the shape of the  $10^\circ$  blade angle shows that the average  $C_p$  increases with the number of blades up to a variation of the number of blades 40, then the average  $C_p$  will decrease. At 250 rpm, the speed of the 12-blade runner with an angle variation of  $10^\circ$   $C_p$  increased again, but then decreased. This appears to be distinct from the phenomena exhibited by other variations, but a line graph reveals the identical pattern. This occurs because it employs speed points with 50 rpm intervals, so there are numerically 50 scales of speed variations that are disregarded with each increase. The 12-blade runner's change in  $C_p$  at each speed adjustment differs slightly from the other runners.

Fig. 10 shows the performance of the turbine Bánki with a blade's angle of  $15^\circ$ . The results show a positive value at the rotational speed interval of 50 – 450 rpm. The  $C_{p_{max}}$  values for each blade sequentially from 8-blades to 52-blades were 0.112, 0.198, 0.183, 0.204, 0.252, 0.307, 0.329, 0.327, 0.235, and 0.203. in general, all variations in the number of blades will reach  $C_{p_{max}}$  at a rotational speed of 200-250 rpm. The 32-blades to 52-blade variations have a longer rotational speed interval than the other variations, up to 450 rpm. In general, the shape of the  $15^\circ$  blade angle shows that the average  $C_p$  increases with the number of blades up to a variation of the number of blades 40, then the average  $C_p$  will decrease.

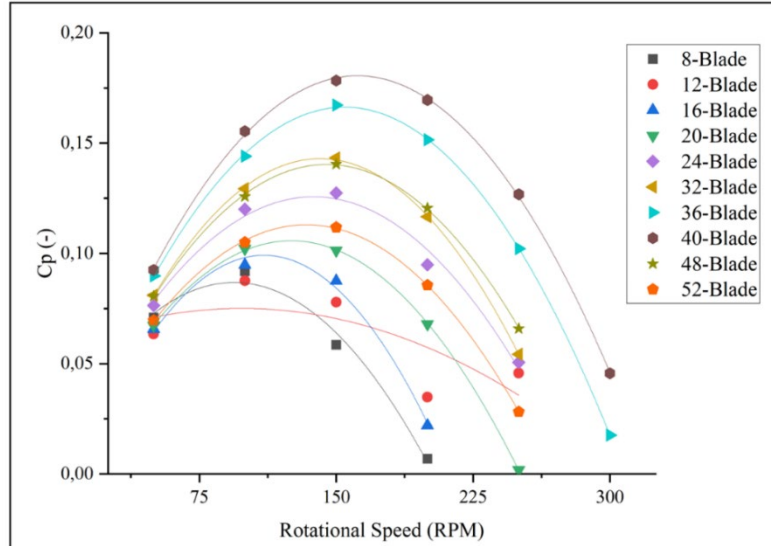


Fig. 9: Graph of  $C_p$  on Blade's Angle  $10^\circ$ .



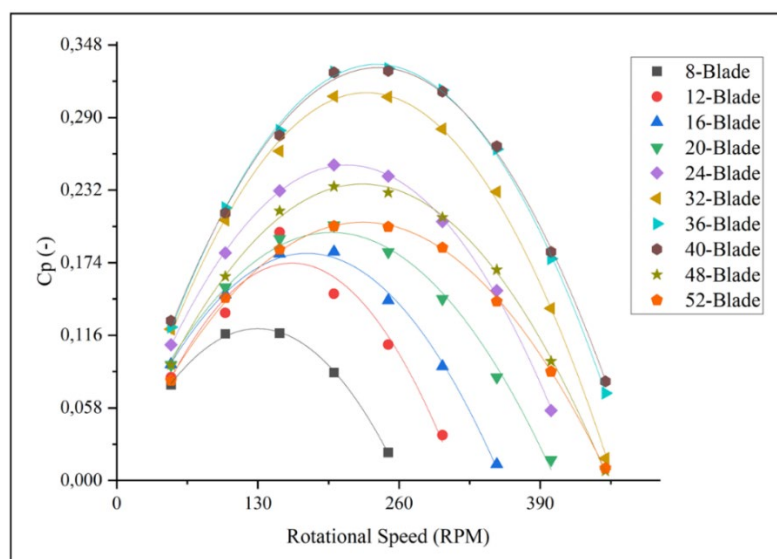
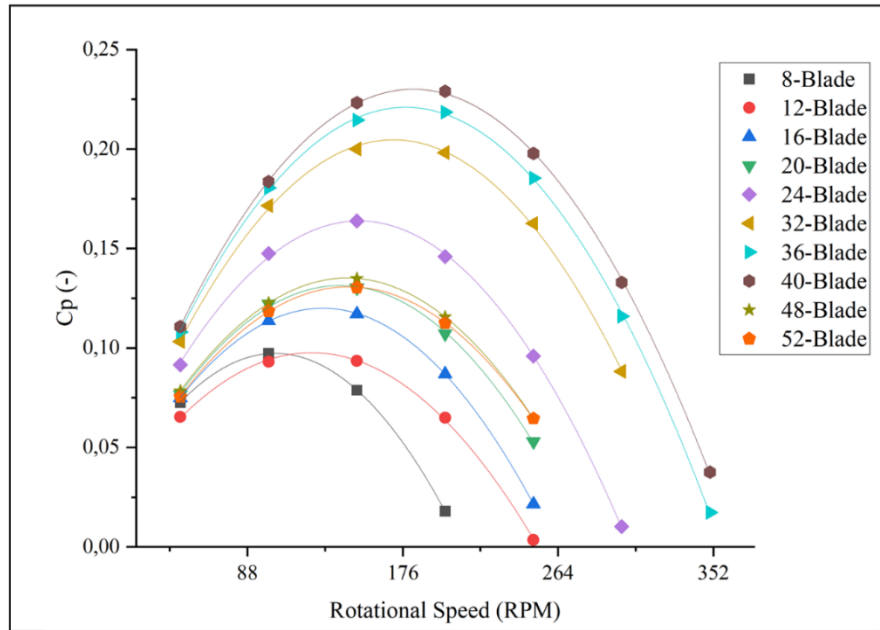


Fig. 10: Graph of Cp on Blade's Angle 15°.

Using a blade angle of 20°, Fig. 11 demonstrates the efficiency of the turbine Bánki. Specifically, between 50 and 350 revolutions per minute, the results are positive. From eight blades to fifty-two blades, the  $C_{p_{max}}$  values obtained were 0.097, 0.094, 0.117, 0.130, 0.164, 0.20, 0.218, 0.229, 0.135, and 0.130. At a speed of 150 revolutions per minute,  $C_{p_{max}}$  is reached for all practical purposes across a wide range of blade counts. The 36-bladed and 40-bladed variants can rotate at speeds of up to 350 rpm, which is significantly higher than the speeds of the other variants. The general form of the graph at a blade angle of 20° demonstrates that the average Cp rises with an increase in the number of blades up to a variation in the number of blades of 40, and then falls off.

The performance of the turbine Bánki with a 25° blade angle is shown in Fig. 12. At the range of 50 to 350 rpm, the results indicate a positive value. From 8 blades to 52 blades, the  $C_{p_{max}}$  values were 0.097, 0.17, 0.129, 0.145, 0.178, 0.226, 0.247, 0.248, 0.156, and 0.141 for each blade in turn. The  $C_{p_{max}}$  will typically be reached for all

variations in the number of blades at a rotational speed of between 150 and 200 rpm. The rotational speed interval of the 36 to 40-blade variations is 350 rpm, which is higher than that of the other variations. The average Cp increases with an increase in the number of blades up to a variation in the number of blades of 40, then decreases after that, according to the shape of the 25-degree blade angle. Fig. 13 shows the performance of the turbine Bánki with a blade angle of 30°. The results show a positive value at the rotational speed interval of 50 – 400 rpm. The  $C_{p_{max}}$  values for each blade sequentially from 8-blades to 52-blades were 0.097, 0.112, 0.140, 0.157, 0.20, 0.25, 0.267, 0.255, 0.157, and 0.157. In general, all variations in the number of blades will reach  $C_{p_{max}}$  at a rotational speed of 150 rpm and 200 rpm. The 32-blades to 40-blades variations have a longer rotational speed interval than the other variations, up to 400 rpm. In general, the shape of the 30° blade angle shows that the average Cp increases with the number of blades up to a variation of the number of blades 36, then the average Cp will decrease.



**Fig. 11:** Graph of Cp on Blade's Angle 20°

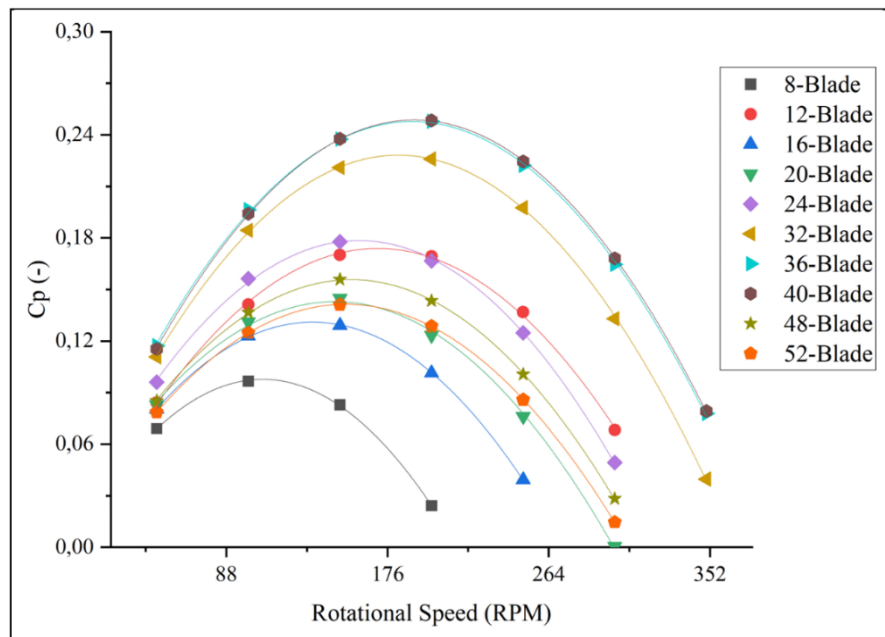


**Fig. 12:** Graph of Cp on Blade's Angle 25°.



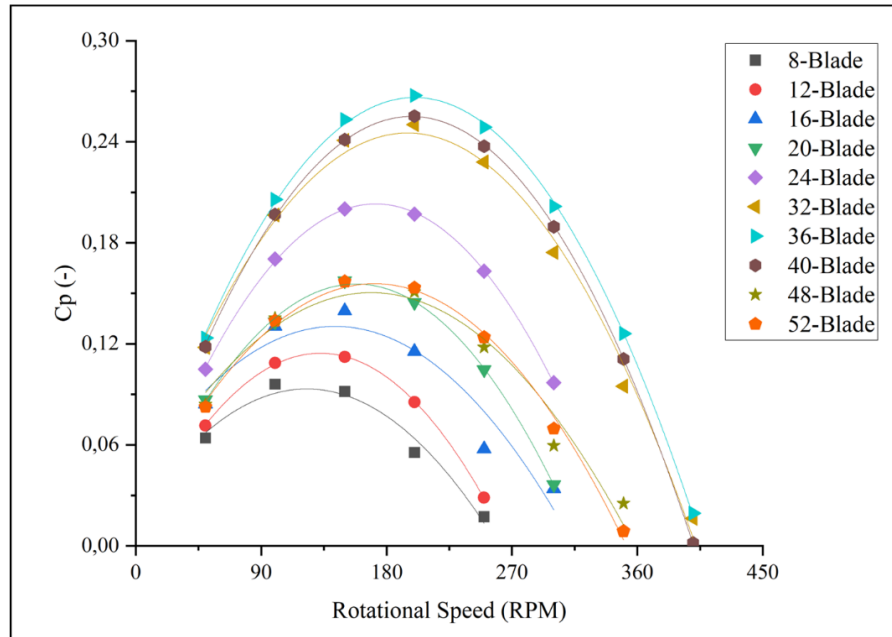


Fig. 13: Graph of  $C_p$  on Blade's Angle  $30^\circ$ .

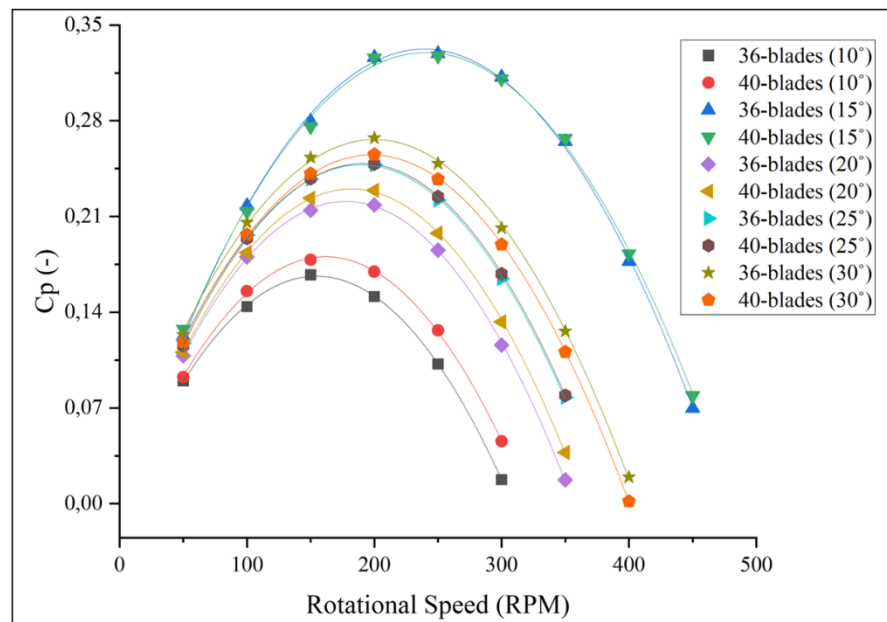


Fig. 14: Graph of  $C_p$  on Bánki turbine 36-blades and 40-blade with blade's Angle Variation.

The effect of the number of blades in this study shows that there is an increase in  $C_{p_{\max}}$  as the number of blades increases up to 40-blades for all variations of blade angles. This is similar to experimental studies that have been conducted on 15-blade to 25-blades that experienced an increase in  $C_{p_{\max}}$  in various shapes and blade angles<sup>32</sup>. In this study, the performance decreased after the 40-blade variation, where in this study the maximum number of blades was obtained to obtain  $C_{p_{\max}}$ .

Fig. 14 shows the performance of the Turbine Bánki on 36-blades and 40-blades with variations of the blade angles of  $10^\circ$ ,  $15^\circ$ ,  $20^\circ$ ,  $25^\circ$ , and  $30^\circ$ . The results show positive values in the rotational speed interval of 50 – 450 rpm.  $C_{p_{\max}}$  is generally achieved at a rotational speed of

200 rpm. The  $15^\circ$  variation has a longer rotational speed interval than the other variations up to 450 rpm.

In Fig. 15, the pressure contour is displayed. The 40-blade runner produces the best  $C_{p_{\max}}$  overall, so angle variations on this runner produce the pressure contour. However, at  $10^\circ$ , the pressure area is yellow (high pressure), and it is situated on the inner diameter of the narrow runner (which is smaller) than the area of the other angle variations. Generally speaking, the pressure contours are similar. Therefore, in terms of the torque, results indicate little impact. Compared to different angle variations, the pressure contour on the inner diameter is more evenly distributed at  $15^\circ$ . The velocity contour is shown in Fig. 16, and the velocity vector is shown in Fig.

17. From the speed contour, the Runner with an angle of  $15^\circ$  has a more apparent wake zone than the other variations. However, because it is located on the back side of the blade, it makes the Runner more flexible to return to its initial position (spin). This phenomenon benefits the Runner because it produces greater torque.

The last step in the research that has been done is to perform statistical analysis using the factorial design method. This analysis uses two factors: the blade angle factor and the number of blades. The results of the research are shown in Table 3. The  $F_0$  value in Table 3 will be compared with the  $F_{table}$  value in Table 4. The Blade's Angel factor shows that  $F_0 > F_{table}$ . The number of blades factor on the Runner also offers the same thing that  $F_0 > F_{table}$ . The results of the analysis show that there is an interaction between the blade's angel factor and the number of blades. This concept can be extended to parametric study of other renewable energy harvests, such as, wind turbine and photovoltaic<sup>33-37</sup>).

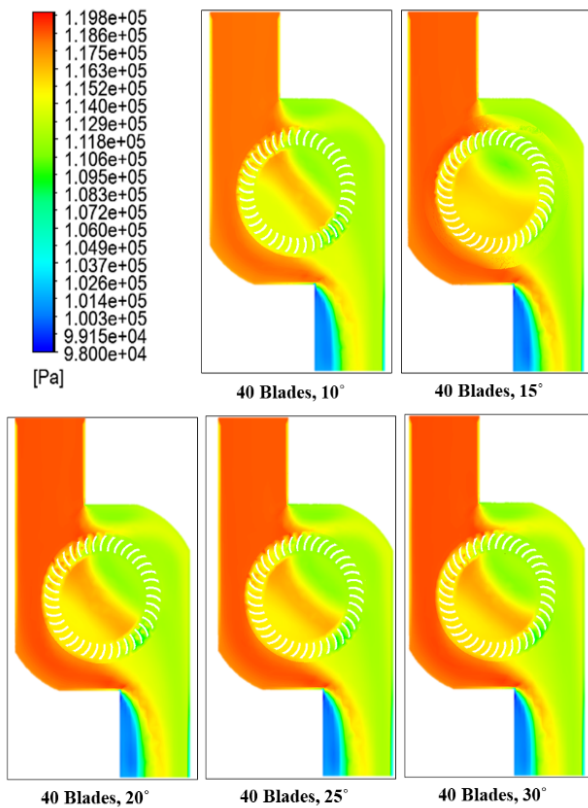


Fig. 15: Pressure Contour on Bánki Turbine 40-blades.

Source of Variation	Sum of Squares	DOF	Mean Square	$F_0$
Blade's Angle	0.086	4	0.0200	110.04
Number of Blades	0.126	11	0.0100	58.80
Interaction	0.007	1	0.0066	34.05
Error	0.008	43	0.0002	
<b>Total</b>	<b>0.230</b>	<b>59</b>		

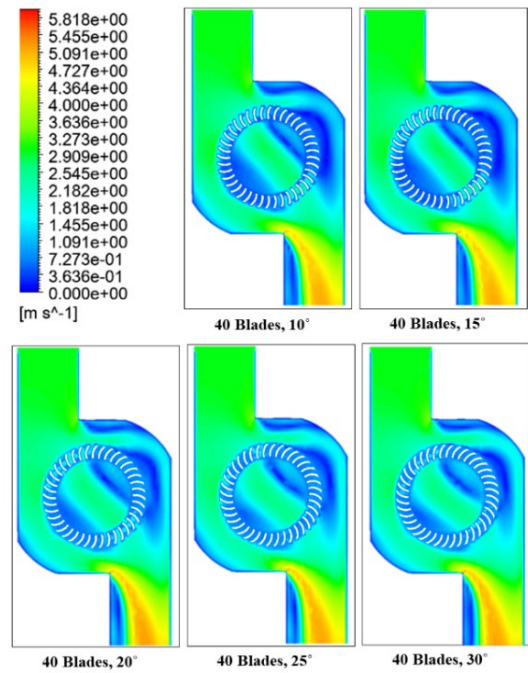


Fig. 16: Velocity Contour on Bánki Turbine 40-blades.

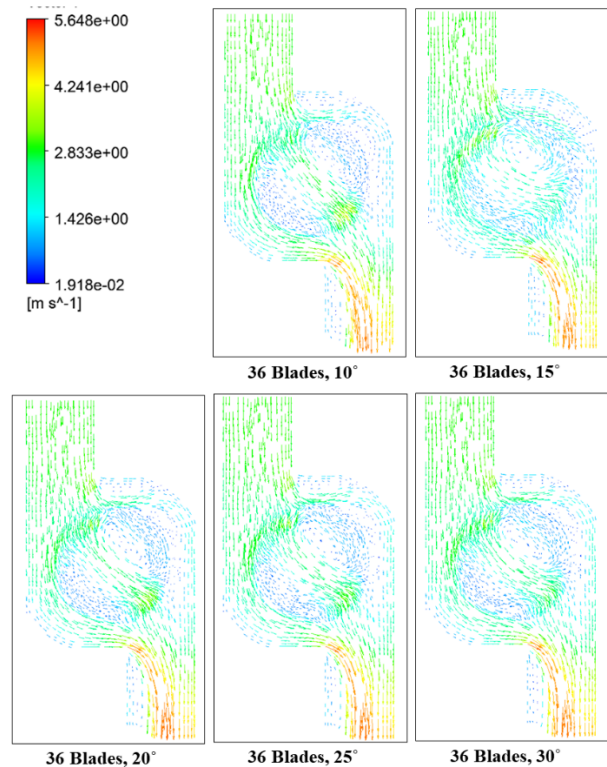


Fig. 17: Velocity Vector on Bánki Turbine 40-blades.

Table 4.  $F_0$  distribution Value [15].

$\alpha = 0.01$			
Degrees of Freedom	$V_1 (0.01)$		
	1 (Interaction)	4 (Blade's Angle)	11 (Number of blades)
59	7.08	3.65	2.5

## 6. Conclusions

In the validation process, 3D modeling of the Bánki Turbine was completed with a 6% error. According to the results, blade angles of 10°, 15°, 20°, and 25° produce  $C_{p_{max}}$  on the 40-blade Runner, while blade angles of 30° produce  $C_{p_{max}}$  on the 36-blade Runner. Overall, runners with 40-blades produce the highest  $C_{p_{max}}$ . This demonstrates that the number of 40-blades represents the maximum number of blade throughout the variation of the angle, as the 40-blade's narrow gap between blade creates a smaller wake zone than the other blade's numbers. The Blade Angle factor demonstrates that a blade with an angle of 15° produces the best  $C_{p_{max}}$  for all number of blade variations.

The analysis using a factorial design shows that the Blade's Angle factor and the number of blades significantly affect the resulting Cp. The Blade's Angle factor has a more significant influence than the number of blade factors. The analysis also reveals an interaction between the angle factor of the blade and the number of blades. The results showed that the  $C_{p_{max}}$  that could be chilled was 0.327 at a rotational speed of 250 rpm. These results were obtained at the 15° blade angle and 40-blades Runner variation. So the design with these variations is a good alternative for runners to get maximum performance.

Research will continue with the goal of improving other geometries, such as the runner design's blade profile, which currently has a 15° blade angle and 40 blades. To achieve this goal, we employ alternative designs that exhibit enhanced performance. As a result, Bánki is becoming more effective at transforming energy.

## Acknowledgements

This research was funded by Universitas Sebelas Maret under funding scheme "Penelitian Unggulan Terapan" (PUT-UNS) year 2023 with contract/grant number 228/UN27.22/PT.01.03/2023. The grant is gratefully acknowledged by authors.

## Nomenclature

$A$	Area Swept by the Runner ( $m^2$ )
$CFD$	Computational Fluid Dynamics
$C_p$	Coefficient of power (-)
$C_{p_{max}}$	Coefficient of power - maximum (-)
$C_t$	Coefficient of torque (-)
$D_1$	Inner Diameter Runner (mm)
$D_2$	Outer Diameter Runner (mm)
$DOF$	Degree of Freedom
$FDA$	Factorial Design Analysis
$F_0$	Ratio of the sample variances
$F_{table}$	Percentage Points of the F Distribution
$n$	Power (W)
$P_{available}$	Power available (W)

$P_{runner}$	Power runner (W)
$Rpm$	Revolutions per minute
$R_r$	Radius (mm)
$SS$	Sum of squares
$T$	Torque (Nm)
$TSR$	Torque-speed ratio (-)
$t$	Thickness (mm)
$V$	Velocity Inlet (m/s)
$\nu_1$	Degrees of Freedom for the Numerator 1
$\nu_2$	Degrees of Freedom for the Numerator 2

## Greek symbols

$\alpha$	Random error
$\rho$	Density ( $kg/m^3$ )
$\theta$	Blade's Angle (°)

## References

- 1) Badan Pengkajian dan Penerapan Teknologi, "Outlook Energi Indonesia 2020", BPPT, 2021 (*In Indonesian*).
- 2) D.M. Prabowoputra, A.R. Prabowo, A. Bahatmaka, and S. Hadi. "Analytical Review of Material Criteria as Supporting Factors in Horizontal Axis Wind Turbines Effect to Structural Responses," *Procedia Structural Integrity*, **27** 155–162 (2020). doi: 10.1016/j.prostr.2020.07.021.
- 3) E. Quaranta, J.P. Perrier, and R. Revelli. "Optimal design process of cross-flow Bánki turbines: Literature review and novel expeditious equations," *Ocean Engineering*, **257** 111582 (2022). doi: 10.1016/j.oceaneng.2022.111582.
- 4) A.R. Prabowo, and D.M. Prabowoputra. "Investigation on Savonius turbine technology as harvesting instrument of non-fossil energy: Technical development and potential implementation," *Theoretical & Applied Mechanics Letters*, **10** 262–269 (2020). doi: 10.1016/j.taml.2020.01.034.
- 5) D.M. Prabowoputra, and A.R. Prabowo, "Effect of Geometry Modification on Turbine Performance: Mini-Review of Savonius Rotor," *International Journal of Mechanical Engineering and Robotics Research*, **11** (10) 777–783 (2022). doi: 10.18178/ijmerr.11.10.777-783.
- 6) M. Naseem, A. Saleem, and M.S. Naseem. "Investigation of blade design parameters for performance improvement of hydraulic cross flow turbine," *Ocean Engineering*, **257** 111663 (2022). doi: 10.1016/j.oceaneng.2022.111663.
- 7) T. Wang, T. Yamagata, and N. Fujisawa. "Effect of blade profile on the efficiency of a waterfall cross-flow hydro turbine," *Energy for Sustainable Development*, **70** 23–31 (2022). doi: 10.1016/j.esd.2022.07.004.
- 8) Purwanto, Budiono, Hermawan, and D.M.

- Prabowoputra, "Simulation Study on Cross Flow Turbine Performance with an Angle of 20 ° to the Variation of the Number of Blades," *International Journal of Mechanical Engineering and Robotics Research*, **11** (1) 31-36 (2022). doi: 10.18178/ijmerr.11.1.31-36.
- 9) M.I. Nadhief, D.M. Prabowoputra, S. Hadi, and D.D.D.P. Tjahjana. "Experimental Study on the Effect of Variation of Blade Arc Angle to the Performance of Savonius Water Turbine Flow in Pipe," *International Journal of Mechanical Engineering and Robotics Research* **9** (5) 779-783 (2020). doi: 10.18178/ijmerr.9.5.779-783.
  - 10) S. Leguizamon, and F. Avellan. "Computational parametric analysis of the design of cross-flow turbines under constraints," *Renewable Energy*, **159** 300-311 (2020). doi: 10.1016/j.renene.2020.03.187.
  - 11) C. A. Mockmore, and F. Merryfield. "The Bánki Water Turbine," Corvallis, Or. : Oregon State College, Engineering Experiment Station, 1949.
  - 12) D.M. Prabowoputra, A. Sartomo, and Suyitno. "The effect of pressure and temperature on biodiesel production using castor oil," *AIP Conference Proceedings*, **2217** 030051 (2020). doi: 10.1063/5.0000504.
  - 13) G. Mehr, M. Durali, M.H. Khakrand, and H. Hoghooghi. "A novel design and performance optimization methodology for hydraulic Cross-Flow turbines using successive numerical simulations," *Renewable Energy*, **169** 1402-1421 (2021). doi: 10.1016/j.renene.2021.01.090.
  - 14) Y.D. Herlambang, Supriyono, B. Prasetyo, and A.S. Alfauzi. "Experimental and Simulation Investigation on Savonius Turbine: Influence of Inlet-Outlet Ratio Using a Modified Blade Shaped to Improve Performance," *Evergreen*, **9** (2) 457-464 (2022). doi: 10.5109/4794172
  - 15) D.M. Prabowoputra, A.R. Prabowo, S. Hadi, and J.M. Sohn. "Assessment of turbine stages and blade numbers on modified 3D Savonius hydrokinetic turbine performance using CFD analysis," *Multidiscipline Modeling in Materials and Structures*, **17** (1) 253-272 (2020). doi: 10.1108/MMMS-12-2019-0224.
  - 16) D.C. Montgomery. "Design and analysis of experiments," John Wiley & Sons, 2017.
  - 17) A. Sartomo, D.M. Prabowoputra, and Suyitno, "Factorial design of the effect of reaction temperature and reaction time on biodiesel production," *AIP Conference Proceedings*, **2217** 030052 (2020). doi: 10.1063/5.0000505
  - 18) K. Thanatwutthikorn, and R. Suntivarakorn, "Optimal Design of Guide Vane for Improving Mini Hydro Power Plant Efficiency by using Twin Axis Vertical Turbine," *International Energy Journal*, **22** (3) 231 – 244 (2022). doi: -
  - 19) D.M. Prabowoputra, and A.R. Prabowo, "Effect of the Phase-Shift Angle on the vertical axis Savonius wind turbine performance as a renewable-energy harvesting instrument," *Energy Reports*, **8** (9) 57-66 (2022). doi: 10.1016/j.egyr.2022.06.092.
  - 20) S. Darmawan, K. Raynaldo, and A. Halim "Investigation of Thruster Design to Obtain the Optimum Thrust for ROV (Remotely Operated Vehicle) Using CFD," *Evergreen*, **9** (1) 115-125 (2022). doi:10.5109/4774224.
  - 21) D.M. Prabowoputra, S. Hadi, A.R. Prabowo, and J.M. Sohn, "Performance Investigation of the Savonius Horizontal Water Turbine Accounting for Stage Rotor Design," *International Journal of Mechanical Engineering and Robotics Research*, **9** (2), 184-189, (2020). doi: 10.18178/ijmerr.9.2.184-189.
  - 22) G. Mehr, M. Durali, M.H. Khakrand, and H. Hoghooghi. "A novel design and performance optimization methodology for hydraulic cross-flow turbines using successive numerical simulations," *Renewable Energy*, **169** 1402-1421 (2021). doi: 10.1016/j.renene.2021.01.090.
  - 23) D.M. Prabowoputra, A.R. Prabowo, S. Hadi, and J.M. Sohn. "The effect of multi-stage modification on the performance of Savonius water turbines under the horizontal axis condition," *Open Engineering*, **10** (1) 793-803 (2020). doi: 10.1515/eng-2020-0085.
  - 24) Warjito, O. Putrawan, Budiarmo, and R. Irwansyah. "The Numerical Study of the Effect of Blade Depth and Rotor-Basin Ratio on Vortex Hydro Turbine Performance," *Evergreen*, **9** (2) 556-562 (2022). doi: 10.5109/4794187.
  - 25) D.M. Prabowoputra, A.R. Prabowo, S. Hadi, and J.M. Sohn. "Performance Assessment of Water Turbine Subjected to Geometrical Alteration of Savonius Rotor," *Proceedings of the 6th International Conference and Exhibition on Sustainable Energy and Advanced Materials - Lecture Notes in Mechanical Engineering*, Springer, 2020. doi: 10.1007/978-981-15-4481-1\_35.
  - 26) D.A. Makarim, D.D.D.P. Tjahjana, Sukmaji I. Cahyono, and S. A. Mazlan. "Performance investigation of the cross-flow water turbine by using CFD," *AIP Conference Proceedings*, **2097** 030083 (2019). doi: 10.1063/1.5098258.
  - 27) R. Luo, H. Zhu, and C. Hu. "Numerical Investigation of an Offshore Overhead Power Transmission System," *Evergreen*, **9** (3) 636-644 (2022). doi: 10.5109/4842521.
  - 28) S. Galvis-Holguin, J.S.D. Rio, and D. Hincapié-Zuluaga. "Enhancement efficiency of Michell-Bánki turbine using NACA 6512 modified blade profile via CFD," *EUREKA: Physics and Engineering*, **2** 55-67 (2022). doi: 10.21303/2461-4262.2022.002351
  - 29) O.M.A.M. Ibrahim, and S. Yoshida. "Experimental and Numerical Studies of a Horizontal Axis Wind Turbine Performance over a Steep 2D Hill," *Evergreen*, **5** (3) 12-21 (2018). doi: 10.5109/1957496

- 30) M. Al-Ghriybah. "Performance Analysis of a Modified Savonius Rotor Using a Variable Blade Thickness," *Evergreen* **9** (3), 645-653 (2022). doi: 10.5109/4842522.
- 31) D.M. Prabowoputra, Purwanto, and Sutini. "The blade's angle affects banki-turbine performance as an alternative design for clean energy generation," *Mathematical Modelling of Engineering Problems*, **10** 259-265 (2023). doi: 10.18280/mmep.100130
- 32) V.R. Desai, and N.M. Aziz. "An experimental investigation of cross-flow turbine efficiency," *Journal of Fluids Engineering*, **116** 545-550 (1994). doi: 10.1115/1.2910311
- 33) D.D.D.P. Tjahjana, Z. Arifin, S. Suyitno, W.E. Juwana, A.R. Prabowo, and C Harsito. "Experimental study of the effect of slotted blades on the Savonius wind turbine performance," *Theoretical and Applied Mechanics Letters*, **11** 100249 (2021). doi: 10.1016/j.taml.2021.100249
- 34) E. Michael, D.D.D.P. Tjahjana, and A.R. Prabowo, "Estimating the potential of wind energy resources using Weibull parameters: A case study of the coastline region of Dar es Salaam, Tanzania," *Open Engineering*, **11** 1093-1104 (2021). doi: 10.1515/eng-2021-0108
- 35) S.D. Prasetyo, A.R. Prabowo, and Z. Arifin, "The use of a hybrid photovoltaic/thermal (PV/T) collector system as a sustainable energy-harvest instrument in urban technology," *Heliyon*, **9** e13390 (2023). doi: 10.1016/j.heliyon.2023.e13390
- 36) S.D. Prasetyo, A.R. Prabowo, and Z. Arifin, "The effect of collector design in increasing PVT performance: Current state and milestone," *Materials Today: Proceedings*, **63** S1-S9 (2022). doi: 10.1016/j.matpr.2021.12.356
- 37) Z. Arifin, S.D. Prasetyo, D.D.D.P. Tjahjana, R.A. Rachmanto, A.R. Prabowo, and N.F. Alfaiz, "The application of TiO<sub>2</sub> nanofluids in photovoltaic thermal collector systems," *Energy Reports*, **8** 1371-1380 (2022). doi: 10.1016/j.egyr.2022.08.070